

## Technical Note: Immunohistochemical evaluation of mouse brain irradiation targeting accuracy with 3D-printed immobilization device

Niloufar Zarghami<sup>a)</sup> and Michael D. Jensen

*Department of Medical Biophysics, The University of Western Ontario, 1151 Richmond Street, London, Ontario N6A 3K7, Canada*

Srikanth Talluri

*Department of Biochemistry, The University of Western Ontario, 1151 Richmond Street, London, Ontario N6A 3K7, Canada and London Regional Cancer Program, London Health Sciences Centre, 800 Commissioners Road East, London, Ontario N6A 5W9, Canada*

Paula J. Foster

*Imaging Research Laboratories, Robarts Research Institute, 100 Perth Drive, London, Ontario N6A 5K8, Canada and Department of Medical Biophysics, The University of Western Ontario, 1151 Richmond Street, London, Ontario N6A 3K7, Canada*

Ann F. Chambers

*Department of Medical Biophysics, The University of Western Ontario, 1151 Richmond Street, London, Ontario N6A 3K7, Canada; Department of Oncology, The University of Western Ontario, 1151 Richmond Street, London, Ontario N6A 3K7, Canada; and London Regional Cancer Program, London Health Sciences Centre, 800 Commissioners Road East, London, Ontario N6A 5W9, Canada*

Frederick A. Dick

*Department of Biochemistry, The University of Western Ontario, 1151 Richmond Street, London, Ontario N6A 3K7, Canada and London Regional Cancer Program, London Health Sciences Centre, 800 Commissioners Road East, London, Ontario N6A 5W9, Canada*

Eugene Wong

*Department of Physics and Astronomy, The University of Western Ontario, 1151 Richmond Street, London, Ontario N6A 3K7, Canada; Department of Medical Biophysics, The University of Western Ontario, 1151 Richmond Street, London, Ontario N6A 3K7, Canada; Department of Oncology, The University of Western Ontario, 1151 Richmond Street, London, Ontario N6A 3K7, Canada; and London Regional Cancer Program, London Health Sciences Centre, 800 Commissioners Road East, London, Ontario N6A 5W9, Canada*

(Received 7 April 2015; revised 23 September 2015; accepted for publication 1 October 2015; published 16 October 2015; corrected 30 October 2015)

**Purpose:** Small animal immobilization devices facilitate positioning of animals for reproducible imaging and accurate focal radiation therapy. In this study, the authors demonstrate the use of three-dimensional (3D) printing technology to fabricate a custom-designed mouse head restraint. The authors evaluate the accuracy of this device for the purpose of mouse brain irradiation.

**Methods:** A mouse head holder was designed for a microCT couch using CAD software and printed in an acrylic based material. Ten mice received half-brain radiation while positioned in the 3D-printed head holder. Animal placement was achieved using on-board image guidance and computerized asymmetric collimators. To evaluate the precision of beam localization for half-brain irradiation, mice were sacrificed approximately 30 min after treatment and brain sections were stained for  $\gamma$ -H2AX, a marker for DNA breaks. The distance and angle of the  $\gamma$ -H2AX radiation beam border to longitudinal fissure were measured on histological samples. Animals were monitored for any possible trauma from the device.

**Results:** Visualization of the radiation beam on *ex vivo* brain sections with  $\gamma$ -H2AX immunohistochemical staining showed a sharp radiation field within the tissue. Measurements showed a mean irradiation targeting error of  $0.14 \pm 0.09$  mm (standard deviation). Rotation between the beam axis and mouse head was  $1.2^\circ \pm 1.0^\circ$  (standard deviation). The immobilization device was easily adjusted to accommodate different sizes of mice. No signs of trauma to the mice were observed from the use of tooth block and ear bars.

**Conclusions:** The authors designed and built a novel 3D-printed mouse head holder with many desired features for accurate and reproducible radiation targeting. The 3D printing technology was found to be practical and economical for producing a small animal imaging and radiation restraint device and allows for customization for study specific needs. © 2015 American Association of Physicists in Medicine. [<http://dx.doi.org/10.1118/1.4933200>]

Key words: small animal irradiation, immobilization device, 3D printing,  $\gamma$ -H2AX immunohistochemistry, microCT

## 1. INTRODUCTION

Approximately half of all cancer patients undergo radiation therapy as a part of their treatment.<sup>1</sup> Over the last few decades, sophisticated radiation treatment planning, delivery, and image guidance have been introduced and are used routinely. The biological responses of tumor and normal tissue to radiation therapy can be investigated using animal models. Accurate simulation of the patient's treatment scenario on small animals in laboratories will facilitate translating experimental results to the clinical setting and help further our understanding of radiobiology.

Many groups have developed sophisticated preclinical radiation devices, which are capable of treating subregional fields using technologies such as on-board cone beam CT (CBCT). Some devices have integrated bioluminescence tomography while others computerized collimators.<sup>2-5</sup> Indeed, these cutting-edge devices have enabled researchers to investigate some of the current radiobiological challenges and deliver more complex dose distribution. However, another challenge for accurate radiation dose delivery on live animals is their setup and positioning. While accuracies for radiotherapy in the human settings have been elucidated,<sup>6</sup> analogous specifications for small animals are not yet available. Radiation treatment is commonly performed on sedated animals, but unconstrained anatomical structures complicate positioning and restraining devices are needed for accurate targeting. Several groups have developed stereotactic holders to improve dose delivery.<sup>7-9</sup> Moreover, sophisticated commercial devices are available for different small-animal imaging machines.<sup>10</sup> While all these stereotactic holders have the same purpose of improving animal positioning, they may lack some features for some small animal radiotherapy treatment situations. Such features may include physiological monitoring, animal warming, and the capability for fine position adjustments.<sup>9</sup> Two studies evaluated the reproducibility of custom-built restrainers using CT image registration rather than measuring the accuracy of the actual radiation beam in the irradiated tissues.<sup>9,11</sup> On SAARP system, two devices were developed to assist with mouse subregional brain radiation.<sup>7,11,12</sup> However, these restrainers were not the focus of these studies and unlike three-dimensional (3D) printing technology, they are not readily shared and modifiable for other small animal radiation units. Commercially available devices have tended to be designed for imaging rather than radiotherapy. More importantly, traditional fabrication methods may not be economical, especially if several customized variations of a stereotactic holder are required. To allow investigators to optimally position the animal for each treatment site and minimize trauma, it is desirable to economically fabricate multiple external holders for small animal radiation therapy.

In this technical note, we introduce a completely 3D-printed mouse head holder for a microCT/RT system. We investigate the feasibility of using 3D printing technology to make a head holder and then evaluate the head holder's capability for precise mouse brain irradiation. The targeting accuracy is verified with half brain irradiation, using fluorescent immunohistochemical staining for phosphorylated histone H2AX,

$\gamma$ -H2AX, a marker for DNA double-strand breaks,<sup>13,14</sup> on frozen mouse brain sections. Used as a sensitive biosimeter,  $\gamma$ -H2AX responses to radiation doses as low as 1.2 mGy.<sup>15</sup> This novel device demonstrates the potential application of 3D printing to small animal experimental platforms.

## 2. METHODS

### 2.A. Head holder design and 3D printing

The stereotactic mouse head holder was designed for the GE eXplore CT 120 (GE Healthcare, Milwaukee, WI, USA) preclinical imaging system rat couch. This unit has been modified to be capable of small animal imaging and irradiation with on-line image guidance and multiple collimated irradiation fields.<sup>2</sup>

To size the stereotactic holder, mouse gross anatomical measurements were done on 6–8 week old C57BL/6 and NU-Foxn1<sup>nu</sup> (Charles River Laboratories, Wilmington, MA) mice. The mouse head holder was designed using AutoCAD 2014 (Autodesk, Inc., San Rafael, CA, USA) [Fig. 1(a)]. The head holder design has integrated anesthesia gas delivery and respiration pillow sensor. The nose cone position can be adjusted according to the size of the mouse snout and connects to a commercially available Mapleson-D (Patterson Scientific, USA) for anesthetic gas. The respiration pillow sensor is placed under the abdomen of the animal and respiration rate can be monitored during the procedure. The mouse incisors are placed in a bite bar inside of the nose cone. The bite bar and two length and position adjustable ear bars immobilize and orient the head in the desired position for a variety of mice size and strains. The 5° inclined bed allows the mouse to be in a neutral position while keeping the head level with the axis of gantry rotation. There are indents for all four paws and the tail of the animal to ensure reproducible setup. A separate hot water circulation blanket is placed below the holder and is wrapped around to be on top of the animal to maintain its body temperature.

The drawing was exported as three separate parts: bed body, nose cone, and bite bar. The stereolithography (.stl) format was imported to ObjectStudio Software (Stratasys, Inc., Rehovot, Israel) to convert the drawing to 3D layer modeling. The fabrication was done with Objet30Pro printer (Stratasys, Inc., Rehovot, Israel), using an ultraviolet cured, acrylic based plastic (VeroWhite Plus). It took approximately 17 h for Object30Pro to construct this model. The total of 263 g VeroWhite Plus and 129 g supporting material was used for the fabrication. The head holder was postprocessed with a water jet to remove excessive supporting materials and the holes were threaded for screws [Fig. 1(b)]. The billing was based on the amount of material used to build the prototype and it costs approximately Cnd\$350 to print this holder. Our mouse head holder design is available for modification and 3D printing.

### 2.B. Mouse brain irradiation

All procedures followed animal care protocols approved by the Animal Use Subcommittee of The University of Western

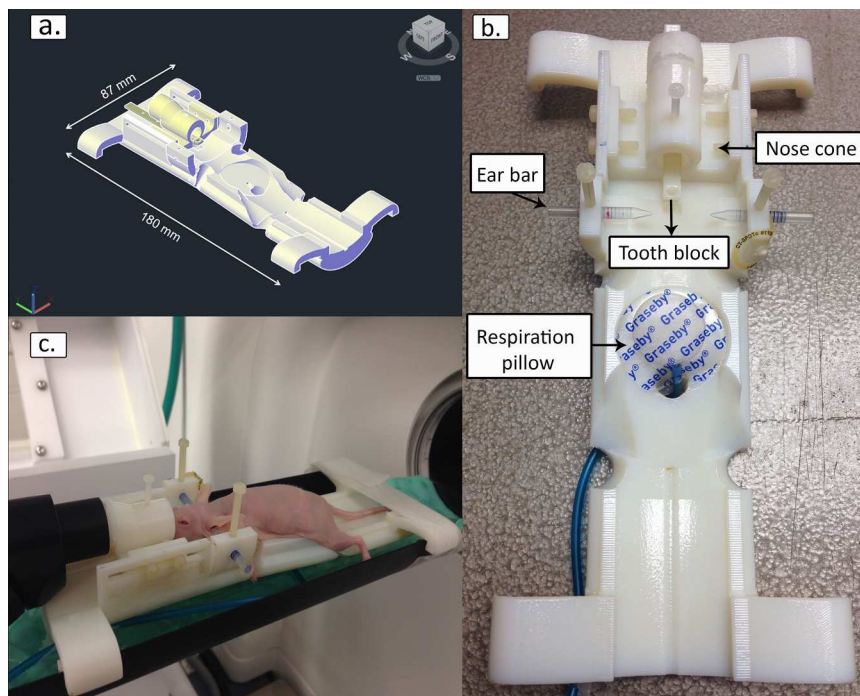


FIG. 1. 3D-printed mouse head holder. (a) Conceptual view of head holder design in AutoCAD™ (2014). (b) Photograph of 3D-printed head holder with integrated respiratory monitoring pillow and adjustable nose cone, tooth bar, and ear bars. (c) Mouse setup in head holder. A water blanket is used on top of the animal for thermal maintenance.

Ontario and were consistent with the policies of the Canadian Council on Animal Care. Mice were anesthetized using 1.5%–2% vaporized inhaled isoflurane while held in the 3D-printed head holder [Fig. 1(c)]. Animals were placed in a feet first prone position inside the scanner. To validate targeting accuracy, the right half of brains from ten adult mice (C57BL/6 or NU-Foxn1<sup>tm</sup>) received the minimum dose of 16 Gy in a single fraction. Longitudinal fissure (LF) was determined as the anatomical target for the edge of the field within the brain. Setup lasers were initially used to set the scanner landmark position relative to the head holder. CT images were used to verify the position of the ear bars and tooth bar [Figs. 2(a) and 2(b)]. Moreover, CT was used to check the mouse head alignment in 3D. Once the mouse was positioned for treatment, online dorsal–ventral fluoroscopy was acquired to identify the skull features and position the collimators. The collimators were moved so the animal body and left hemisphere of the

brain were shielded. A CT small ball bearing (BB) marker was placed on the right side of the head holder to help the user with the animal orientation on CT and fluoroscopy. The right half of the brain was irradiated with a single field ( $14 \times 20 \text{ mm}^2$ ) from the animal's ventral–dorsal direction (Fig. 3).

## 2.C. Immunohistochemistry

Mice were perfused with 0.9% saline containing 4% paraformaldehyde (PFA) approximately 30 min after treatment. Brains were harvested and postfixed in 4% PFA followed by placing them in successive sucrose solution (10%–30%) until the specimen sank to the bottom.<sup>12</sup> Brain samples were embedded in Tissue-Tek OCT Compound (Sakura, Torrance, CA, USA) and frozen. Cyrosectioning of coronal slices was performed with 10  $\mu\text{m}$  slice thickness. Sections were stained for fluorescent  $\gamma\text{H2AX}$  using a well-established

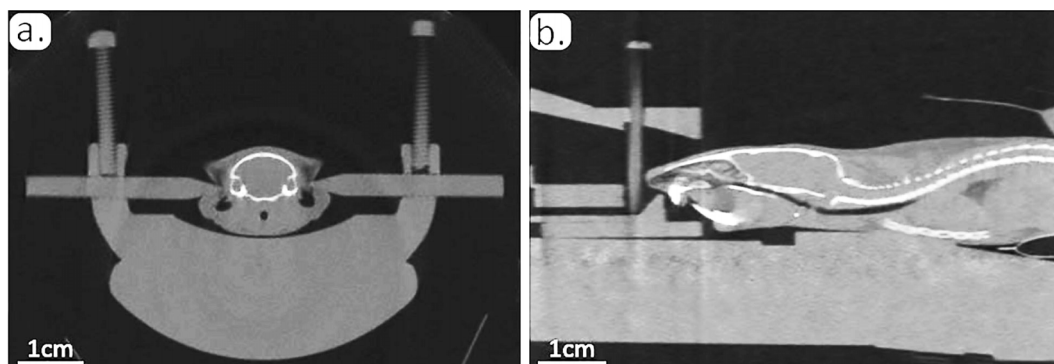


FIG. 2. Pretreatment CT images of the mouse brain positioned in 3D-printed head holder. (a) Coronal view. (b) Sagittal view.

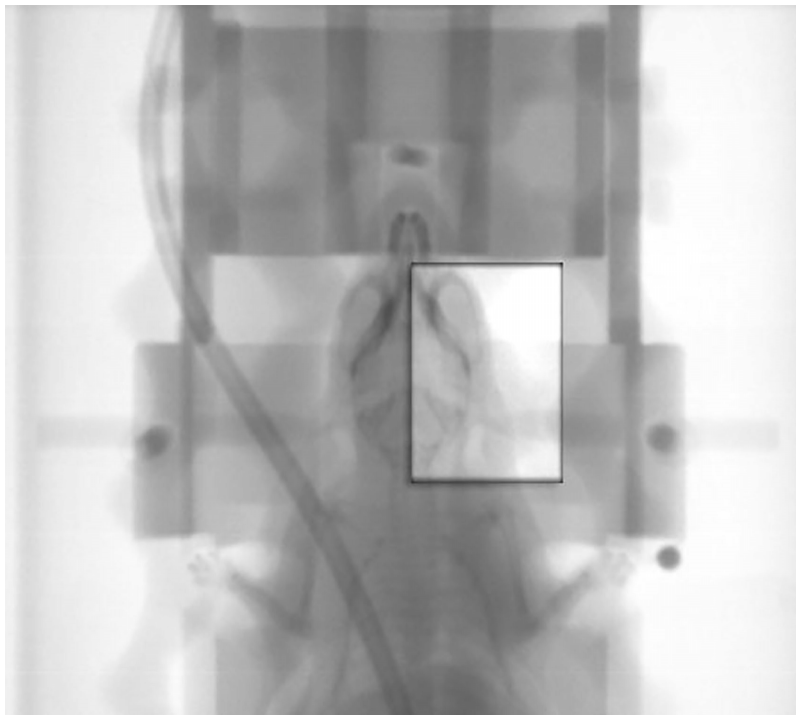


Fig. 3. Beam's eye view fluoroscopy image of the mouse from the top (dorsal–ventral view). Animal is positioned prone in the 3D-printed head holder. The collimated radiation field ( $14 \times 20 \text{ mm}^2$ ) is fused on top of the open field.

protocol published by Ford *et al.*<sup>12</sup> Sections were stained with mouse anti- $\gamma$ -H2AX antibody (antiphosphohistone H2AX, Ser139, clone JBW301; Millipore, Billerica, MA, USA). DNA counterstaining was achieved with incubation in DAPI (4', 6-diamidino-2-phenylindole, Vector Laboratories, Inc., Burlingame, CA). A motorized fluorescent scanning microscope (Leica, Inc.) was used to automatically acquire images with a  $10\times$  objective and stitched them together to form whole brain images on stained histology sections of five mice. To quantify targeting accuracy, another set of  $10\times$  images focusing on the midbrain region were acquired with a fluorescent microscope (Carl Zeiss Canada Ltd.) from all ten mice. All images were acquired under the same microscope settings and exposure parameters.

## 2.D. Analysis

Visualization of the actual beam in tissue was possible using  $\gamma$ -H2AX staining on *ex vivo* brain sections. The  $\gamma$ -H2AX assay has widely been used to demonstrate the localized radiation delivery.<sup>7,12</sup> For targeting accuracy, we measured the distance from the edge of the radiation beam to the intended target (longitudinal fissure) using the digital readout of the fluorescent microscope [Fig. 4(e)]. The edge of the radiation field was visually defined as the border separating cells having enhanced levels of  $\gamma$ -H2AX from those with background staining. The  $\gamma$ -H2AX's penumbra was on the order of tens of microns, which is much smaller than the physical penumbra (0.57–0.73 mm) for this radiation field. The beam offset was measured on two separate histology samples for eight of ten mice and only on one section from the remaining two mice [Figs. 4(a)–4(d)]. To measure the tilt of the animal's head around the rostral–caudal

axis, the angle between longitudinal fissure and the  $\gamma$ -H2AX radiation border was determined on whole brain images in five mice.

## 3. RESULTS

### 3.A. Mouse setup in 3D-printed head holder

Mice were under anesthesia for approximately 1 h and half and breathing rate was monitored during treatment. Mice recovered well from isoflurane after treatment without any signs of trauma to their ears or mouth.

### 3.B. Validating beam targeting accuracy with $\gamma$ -H2AX staining

Immunohistochemical staining of brain sections stained for  $\gamma$ -H2AX showed precise targeting of the field edge at the expected location. The sharp and straight edge of the field through the whole brain for all samples indicates a stable and straight head position around the axis of gantry rotation. The edge of the beam was offset from the longitudinal fissure by a mean distance of  $146 \pm 98 \mu\text{m}$  (standard deviation) toward the left side in ten mice. The average head tilt was determined to be  $1.21^\circ \pm 1^\circ$  (standard deviation) about the axis of the gantry rotation (rostral–caudal), indicating that the x-ray source was positioned slightly toward the right side of the animal (Table I).

## 4. DISCUSSION

We designed, implemented, and verified a 3D-printed mouse head holder.<sup>17</sup> With image guidance and the head holder, we found that the radiation beam edge could be

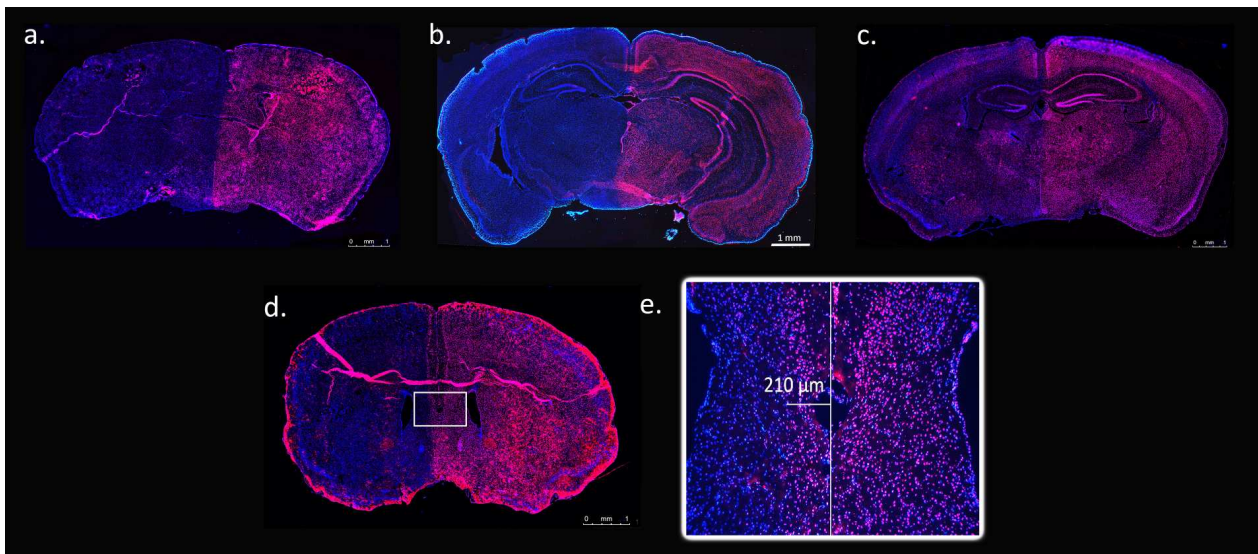


Fig. 4. Fluorescence microscopy of  $\gamma$ -H2AX stained brain sections, imaged at 10 $\times$  magnification and counterstained with DAPI. Sections from four irradiated mice treated in 3D-printed head holder are shown. Intended target was the right half of the brain. (a)–(d) Example measurement of targeting error on zoomed 10 $\times$  image. The bright red line in the middle of brain is due to tissue fold. Distance between longitudinal fissure and  $\gamma$ -H2AX field edge is shown (e).

located within 0.15 mm of the intended target as determined by  $\gamma$ -H2AX immunohistochemical staining of mouse brain sections.

Figure 5 shows the CT examples of two mice treated without the head holder. Variability in the head orientation makes it difficult to collimate and deliver the desired targeted brain irradiation. The corresponding  $\gamma$ -H2AX stained histological sections for these mice showed that the actual radiation beam was offset approximately 2200 and 420  $\mu$ m, respectively, from the midline of the brain. These results led us to design and fabricate the head holder for consistent positioning and setup.

The 3D-printed head holder contains many of the desired features. Its fabrication is more economical than commercial versions and allows for modification according to specific experimental setup.

TABLE I. Targeting accuracy measurement of  $\gamma$ -H2AX stained brain sections. Positive angle indicates an x-ray tube toward the right side of the mouse. Positive offset indicates the radiation beam toward the left side of the longitudinal fissure.

Mouse	Tilt angle (deg)	Offset measurement 1 ( $\mu$ m)	Offset measurement 2 ( $\mu$ m)	Offset mean ( $\mu$ m)
1	1.5	241	211	226
2	0.2	32	26	29
3	2.3	172	190	181
4	N/A	168	191	180
5	0.1	21	48	35
6	N/A	69	52	61
7	N/A	178	200	189
8	N/A	255	N/A	255
9	2.0	280	N/A	280
10	N/A	34	28	31

Note: N/A indicates not available.

One possible limitation of 3D printing is the strength of the material. To overcome the fragility of the material, the base of the head holder was designed thicker (1.5 cm) compared to the other parts. Presence of the bed or ear bars in the path of the x-ray beam may interfere with dose delivery from lateral and ventral directions; therefore, a different design may be needed for treating from other directions.

We validated our targeting accuracy by doing immunohistochemical staining of our samples. Physical changes such as tissue shrinkage and changes in morphology are possible during tissue processing. Wehrl *et al.*<sup>16</sup> measured shrinkage between  $-11.7\%$  and  $30.7\%$  for the PFA fixative depending on the anatomical landmark. Moreover, Ford *et al.*<sup>12</sup> reported the shrinkage factor of 0.85 for the fixed and frozen mouse brain samples. Applying the 0.85 shrinkage factor to our data, the mean beam offset is  $172 \pm 115 \mu$ m.

The 3D-printed head holder assisted with animal positioning; however, the beam offset from the target not only depends on the mouse head alignment but also on the placement of the collimators. In this study, the half brain was determined visually using on-board imaging. Moreover, the 20%–80% radiation penumbra for  $14 \times 20 \text{ mm}^2$  field is estimated to be 0.57–0.73 mm for this system.<sup>2</sup> All histological analyses were done on 10 $\times$  microscope images, which is not suitable for detecting  $\gamma$ -H2AX foci in response to small doses. Only the sharp edge of the beam was detected and the localization may be dependent on microscope and display parameters.

Our results showed that the  $\gamma$ -H2AX fluorescence stains consistently ( $n = 10$ ) past the midline of the brain by 0.146 mm on average (range 0.03–0.28 mm). There are a few possible explanations to this finding. First, in this study, we used fluoroscopy image guidance to place the edge of the radiation field. Ideally, the 50% of the beam penumbra would be at the midbrain. There will be uncertainty with this placement. Moreover,  $\gamma$ -H2AX assay is sensitive to low doses of radiation,<sup>15</sup>

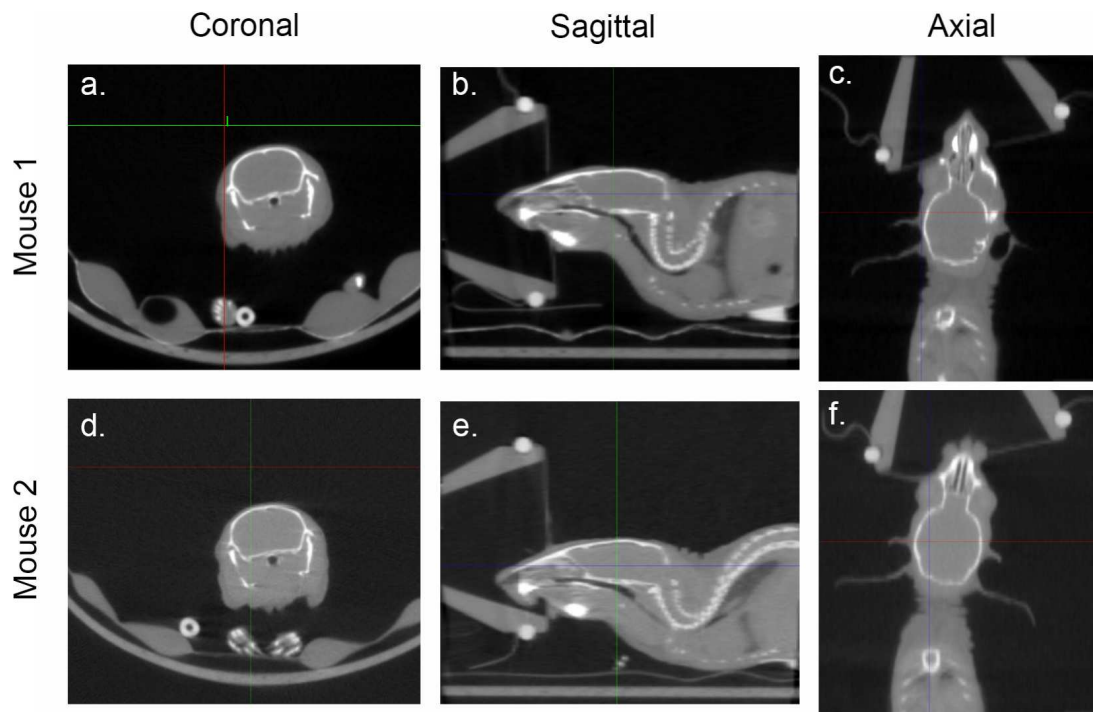


FIG. 5. Pretreatment CT images of two mice irradiated without the 3D-printed head holder, demonstrating variability in setup. Variability in head orientation compared to mice with head holder (Figs. 2 and 3) increased uncertainties in targeted mouse brain irradiation.

therefore, even if the beam edge was placed at the midbrain, the  $\gamma$ -H2AX staining border would shift to the un-irradiated side. Finally, mice were under isoflurane for about an hour and half for setup and treatment, and intrafraction head motion may occur, adding to the uncertainties.

Our designed 3D-printed mouse head holder may not only be applicable to mouse brain irradiation but potentially to other sites. To irradiate other sites of the animal, the head holder model can be redesigned so that less material would be in the way of the radiation beam and reduce the attenuation. With modification in design, our head holder may be a starting point for an even greater range of imaging and radiation preclinical studies.

## 5. CONCLUSIONS

Numerous studies have employed different stereotactic devices. We have demonstrated that a 3D-printed stereotactic head restraint can allow accurate and precise irradiation in a mouse brain. Immunohistochemical  $\gamma$ -H2AX staining validated the irradiation of specific subregions of the mouse brain with less than a millimeter error. Fast 3D-printing technology allowed us to produce a custom stereotactic holder with the necessary features for our study in an economical and timely manner.

## ACKNOWLEDGMENTS

The authors would like to thank John Moore for assistance in operating the 3D-printer. Frank Van Sas and Brian Dalrymple are acknowledged for assistance with postprint-

ing fabrication. The authors thank Tom Hrinivich for helpful discussions and Heather Craig for assistance with the motorized microscope. This work is funded by the Natural Sciences and Engineering Research Council of Canada and London Regional Cancer Program Catalyst Grant and also supported by a Translational Breast Cancer Studentship award to NZ funded in part by the Breast Cancer Society of Canada.

<sup>a)</sup> Author to whom correspondence should be addressed. Electronic mail: nzargham@uwo.ca

<sup>1</sup>C. E. DeSantis, C. C. Lin, A. B. Mariotto, R. L. Siegel, K. D. Stein, J. L. Kramer, R. Alteri, A. S. Robbins, and A. Jemal, "Cancer treatment and survivorship statistics," *Ca-Cancer J. Clin.* **64**(4), 252–271 (2014).

<sup>2</sup>M. D. Jensen, W. T. Hrinivich, J. A. Jung, D. W. Holdsworth, M. Drangova, J. Chen, and E. Wong, "Implementation and commissioning of an integrated micro-CT/RT system with computerized independent jaw collimation," *Med. Phys.* **40**(8), 081706 (13pp.) (2013).

<sup>3</sup>R. Tuli, M. Armour, A. Surmak, J. Reyes, and J. Wong, "Abstract 5725: Accuracy of off-line bioluminescence imaging to localize targets in pre-clinical radiation research," *Cancer Res.* **72**(4), 5725 (2012).

<sup>4</sup>S. J. Van Hoof, P. V. Granton, and F. Verhaegen, "Development and validation of a treatment planning system for small animal radiotherapy: SmART-plan," *Radiother. Oncol.* **109**(3), 361–366 (2013).

<sup>5</sup>R. Clarkson, P. E. Lindsay, S. Ansell, G. Wilson, S. Jelveh, R. P. Hill, and D. A. Jaffray, "Characterization of image quality and image-guidance performance of a preclinical microirradiator," *Med. Phys.* **38**(2), 845–856 (2011).

<sup>6</sup>J. V. Dyk, J. J. Battista, and G. S. Bauman, *Accuracy and Uncertainty Considerations in Modern Radiation Oncology* (The Modern Technology of Radiation Oncology, 2013), pp. 361–412.

<sup>7</sup>B. C. Baumann, J. L. Benci, P. P. Santoiemma, S. Chandrasekaran, A. B. Hollander, G. D. Kao, and J. F. Dorsey, "An integrated method for reproducible and accurate image-guided stereotactic cranial irradiation of brain tumors using the small animal radiation research platform," *Transl. Oncol.* **5**(4), 230–237 (2012).

<sup>8</sup>L. Zhang, H. Yuan, L. M. Burk, C. R. Inscoe, M. J. Hadsell, P. Chtcheprov, Y. Z. Lee, J. Lu, S. Chang, and O. Zhou, "Image-guided microbeam irradiation

- to brain tumour bearing mice using a carbon nanotube x-ray source array," *Phys. Med. Biol.* **59**(5), 1283–1303 (2014).
- <sup>9</sup>E. L. Kiehl, S. Stojadinovic, K. T. Malinowski, D. Limbrick, S. C. Jost, J. R. Garbow, J. B. Rubin, J. O. Deasy, D. Khullar, E. W. Izaguirre, P. J. Parikh, D. A. Low, and A. J. Hope, "Feasibility of small animal cranial irradiation with the microRT system," *Med. Phys.* **35**(10), 4735–4743 (2008).
- <sup>10</sup>D. W. Holdsworth, S. A. Detombe, C. Chiodo, S. T. Fricke, and M. Drangova, "Implementation and assessment of an animal management system for small-animal micro-CT/micro-SPECT imaging," *Proc. SPIE* **7965**, 79650N-1–79650N-6 (2011).
- <sup>11</sup>M. Armour, E. Ford, I. Iordachita, and J. Wong, "CT guidance is needed to achieve reproducible positioning of the mouse head for repeat precision cranial irradiation," *Radiat. Res.* **173**(1), 119–123 (2010).
- <sup>12</sup>E. C. Ford, P. Achanta, D. Purger, M. Armour, J. Reyes, J. Fong, L. Kleinberg, K. Redmond, J. Wong, M. H. Jang, H. Jun, H.-J. Song, and A. Quinones-Hinojosa, "Localized CT-guided irradiation inhibits neurogenesis in specific regions of the adult mouse brain," *Radiat. Res.* **175**(6), 774–783 (2011).
- <sup>13</sup>D. R. Pilch, O. A. Sedelnikova, C. Redon, A. Celeste, A. Nussenzweig, and W. M. Bonner, "Characteristics of gamma-H2AX foci at DNA double-strand breaks sites," *Biochem. Cell Biol.* **81**, 123–129 (2003).
- <sup>14</sup>E. P. Rogakou, D. R. Pilch, A. H. Orr, V. S. Ivanova, and W. M. Bonner, "DNA double-stranded breaks induce histone H2AX phosphorylation on serine 139," *J. Biol. Chem.* **273**(10), 5858–5868 (1998).
- <sup>15</sup>K. Rothkamm and M. Löbrich, "Evidence for a lack of DNA double-strand break repair in human cells exposed to very low x-ray doses," *Proc. Natl. Acad. Sci. U. S. A.* **100**(9), 5057–5062 (2003).
- <sup>16</sup>H. F. Wehrli, I. Bezrukov, S. Wiehr, M. Lehnhoff, K. Fuchs, J. G. Mannheim, L. Quintanilla-Martine, U. Kohlhofer, M. Kneilling, B. J. Pichler, and A. W. Sauter, "Assessment of murine brain tissue shrinkage caused by different histological fixatives using magnetic resonance and computed tomography imaging," *Histol. Histopathol.* **30**(5), 601–613 (2015).
- <sup>17</sup>See supplementary material at <http://dx.doi.org/10.1118/1.4933200> for the mouse head holder AutoCad design.